IEEE Access
Multidisciplinary ⋮ Rapid Review ⋮ Open Access Journal

Received March 1, 2022, accepted April 7, 2022, date of publication April 13, 2022, date of current version April 19, 2022.

Digital Object Identifier 10.1109/ACCESS.2022.3167051

Novel Successive Interference Cancellation (SIC) With Low-Complexity for GFDM Systems

BEHZAD MOZAFFARI TAZEHKAND[1], MOHAMMAD REZA GHAVIDEL AGHDAM[1], VIDA VAKILIAN[2], AND REZA ABDOLEE[2]

[1]Faculty of Electrical and Computer Engineering, University of Tabriz, Tabriz 5166616471, Iran
[2]Department of Computer Science, California State University Channel Islands, Camarillo, CA 93012, USA

Corresponding author: Behzad Mozaffari Tazehkand (mozaffary@tabrizu.ac.ir)

This work was supported by the NSF ERAS Award ECCS-2029973.

ABSTRACT Generalized frequency-division multiplexing (GFDM) is one of the promising multi-carrier modulation schemes suitable for next-generation wireless communication systems. The main characteristic of GFDM is the flexible time-frequency structure of data blocks. However, this degree of freedom is obtained at the cost of loss of sub-carrier orthogonality, which leads to self-interference. In this paper, we propose a new model that classifies the GFDM self-interferences into two independent categories as inband and adjacent sub-carriers interferences and show their corresponding mathematical formulations. Building on this model, we propose a successive interference cancellation (SIC) technique with low complexity to eliminate these self-interference effectively. The main distinct feature of our proposed technique is its low computational complexity compared to similar interference cancellation techniques. Our analytical findings and numerical experiments indicate that the proposed model and SIC technique considerably improve the system performance in terms of bit error rate (BER) and signal to interference ratio (SIR). We also show that the results of our analytical findings are in good agreement with those of computer simulations.

INDEX TERMS 5G, GFDM, multi-carrier, SIC, BER.

I. INTRODUCTION

Orthogonal frequency division multiplexing (OFDM) is still one of the popular waveform technologies of today's wireless communication systems [1]. The two main features of OFDM are the use of cyclic prefix (CP) to overcome multipath fading and the ease of implementation thanks to fast Fourier transform (FFT) [2], [3]. However, there are some drawbacks in OFDM systems, such as the spectrum inefficiency because of long CP length, high peak to average power ratio (PAPR) due to the multicarrier scheme structure and out-of-band leakage (OOB) [4], [5]. In addition, OFDM systems require strict synchronization to keep orthogonality between sub-carriers [6], and they are sensitive to time and frequency shift, which calls for more signal processing and precise hardware implementation to prevent performance degradation [7], [8].

To support emerging applications with various constraints, such as Internet of Things (IoT) and machine to machine (M2M) communications, fifth-generation (5G) wireless communication systems and beyond require massive concurrent access, high energy efficiency, and low latency [9]. To fulfill these requirements and overcome some of the problems in OFDM, new multicarrier technologies such as multi-carrier faster-than-Nyquist (MFTN), universal filtered multicarrier (UFMC), filter bank multicarrier (FBMC), and generalized frequency division multiplexing (GFDM) have been proposed [10]–[14].

MFTN improves bandwidth by compressing the Nyquist interval of the signaling pulse in the time domain and the minimum orthogonal frequency separation in the frequency domain. In this waveform, there are both inter-carrier interference (ICI) and inter-symbol interference (ISI) that are created by the time-frequency packing. This leads to high complexity and may limit the practical applications of MFTN [10]. To resolve the issue and improve the MFTN performance, successive interference cancellation (SIC) was proposed in [11].

GFDM is based on the modulation of independent blocks, where each block consists of several sub-carriers with several sub-symbols. The sub-carriers are filtered with a prototype filter that is circularly shifted in time and frequency domain [15]. This process reduces the OOB emissions,

The associate editor coordinating the review of this manuscript and approving it for publication was Wei-Wen Hu.

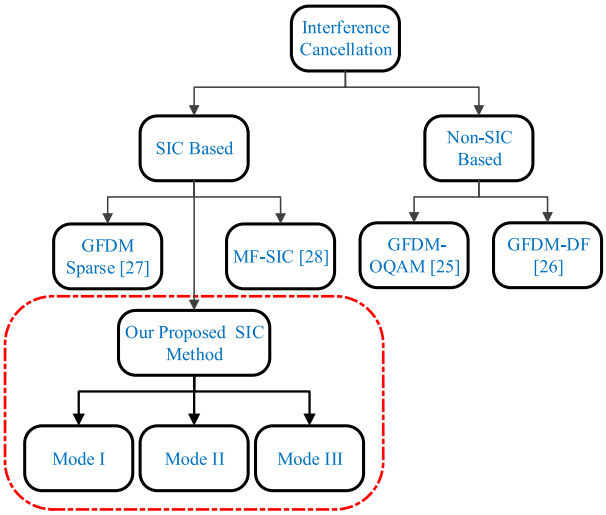

FIGURE 1. Classifcation of interference cancellation techniques.

making fragmented spectrum and dynamic spectrum allocation feasible without severe interference in incumbent services or other users [16]. The CP insertion method of GFDM is spectrally more efficient than that of OFDM because a CP is added to each block consisting of multiple sub-symbols. This will also lead to lower latency in GFDM systems [17].

Nevertheless, GFDM has some drawbacks. It uses a pulse-shaping filter that may cause sub-carriers to become non-orthogonal leading to ICI and ISI [18], [19]. To reduce ICI and ISI, some linear receivers such as zero-forcing (ZF) and minimum mean square error (MMSE) can be used [20], [21]. MMSE offers a good balance between noise filtering and interference reduction, but it is very computationally intensive. The ZF method amplifies noise and degrades bit error rate (BER) performance. In GFDM, SIC can be an effective technique to avoid noise amplification and still achieve a good tradeoff between computational complexity and performance efficiency. The use of the SIC technique in GFDM means the elimination of interference between sub-symbols, which is an idea derived from the NOMA method [22]. In [23] and [24], a new multi-carrier scheme has been introduced that combines GFDM and NOMA techniques.

To put our work into perspective, we classify the interference cancellation methods in GFDM into two categories, namely, SIC-based methods and non-SIC-based methods (See Fig. 1). In non-SIC based, there are GFDM with offset quadrature amplitude modulation (OQAM) [25] and GFDM with dual-filter (GFDM-DF) transceiver [26] methods. The GFDM-OQAM can practically eliminate the signal distortion caused by intrinsic self-interference, but it may not be amenable to practical complex channels [25]. In [26], the two prototype filters are utilized for even and odd sub-carriers separately. This method eliminates the self-interference from the adjacent sub-carriers but increases the OOB of the systems because of using block interleaving.

In SIC-based methods, self-interferences are eliminated at the expense of an increase in computational cost [27], [28]. In [27], the authors have proposed a low-complex GFDM design that uses the SIC technique with a sparse representation of the pulse-shaping filter in the frequency domain by using FFT processing blocks. A GFDM-match filter (MF) system based on SIC with circular pulse-shaping has been introduced in [28]. Although both methods perform well, their computational complexity is still relatively high. In [29], an iterative detection algorithm based on factor graphs estimating complex-valued data symbols transmitted by a GFDM system was proposed and the main drawback of this method is its very high computational complexity.

To improve the performance of GFDM and reduce the computational complexity, we propose a new system model featuring a low complexity SIC technique. Specifically, we define two types of self-interferences in GFDM that we call inband interference and adjacent sub-carriers interference. The inband interference is created due to the frequency interference of sub-symbols within a sub-carrier. The non-orthogonal shapes of the shifted pulses are the cause of the problem in this case. The second type of interference, adjacent sub-carrier interference, is caused by side lobes of the frequency pulse shapes. Based on these two types of self-interferences, we propose a low-complexity SIC technique with the capability of so-called self interferences elimination in GFDM systems. We simultaneously consider the symbol-frequency domain in our formulation that uses the concept of a deterministic modulation matrix. In our proposed model, the system can operate in three modes based on the self-interference type. Mode-I is activated when both inband and adjacent subcarrier interference are present. If the system suffers only from adjacent subcarrier interference, Mode- II is used and Mode-III is activated when only inband interference is present. We can summarize the contribution of our paper as follows:

- We introduce a new system model to represent GFDM signals and analyze different components of the self-interferences in this waveform. We learn that there are two types of self-interferences in the system that are independent of each other and use this feature to design a new SIC technique. We call these interferences inband and adjacent sub-carriers interference for the first time.
- We show how and why Gaussian distribution can be used to model the self-interferences in the system and derive analytical expressions to represent their impact. Our computer experiments validate the correctness of our analytical model.
- We propose a low-complexity SIC technique based on our newly introduced idea of inband interference and adjacent sub-carriers interference and the fact that these interferences are independent. The proposed SIC technique can function in three different modes depending on the source and volume of interferences experienced by the system.

- We derive analytical expressions to evaluate the BER of the system and make comparisons with the recent counterparts in the literature. We also analyze our proposed method in terms of signal-to-noise plus interference ratio (SNIR). We conduct computer simulations to verify the analytical results. Our results show that the analytical results are in good agreement with those of computer simulations.

The rest of the paper is organized as follows. In Section II, we describe the GFDM system model. In Section III, we investigate the self-interference in the GFDM system and provide analytical expressions in Section IV. We discuss the self-interference cancellation method in Section V. The numerical results and complexity analysis are discussed in Section VI, and the conclusion of the paper is presented in Section VII.

II. SYSTEM MODEL

The GFDM transceiver is shown in Fig. 2. First, the modulated data bits are divided into M sub-symbols and K sub-carriers. The total number of data symbols is $N = M \times K$. Then an N point upsampling is applied to the data symbols. Each data symbol is transmitted based on a pulse shape $g[n]$. The output signal without CP can be expressed as:

$$x[n] = \sum_{m=0}^{M-1} \sum_{k=0}^{K-1} d_{k,m} g_{k,m}[n], \quad n = 0, \ldots, N-1, \tag{1}$$

where $g_{k,m}[n] = g[(n - mK) \bmod N] e^{-j2\pi \frac{kn}{K}}$, and n denotes the sampling index and $d_{k,m}$ are the complex-valued data symbol carried by the k^{th} sub-carrier and m^{th} sub-symbol. Each $g_{k,m}[n]$ is a time and frequency shifted version of a prototype filter $g[n]$, where the modulo operation makes $g_{k,m}[n]$ a circularly shifted version of $g_{0,m}[n]$ and the complex exponential performs the shifting operation in frequency [30]. In matrix form, (1) can be expressed as:

$$\mathbf{x} = \mathbf{A}\mathbf{d}, \tag{2}$$

where $\mathbf{A}$ is the GFDM modulation matrix of order $N \times N$ with a structure according to pulse shaping filter $g[n]$ and $\mathbf{d}$ denotes data symbols in a vector form. See (3), as shown at the bottom of the page, for detailed structure.

As shown in Fig. 2, we study the GFDM modulator/demodulator and not the modulation type. The proposed method is independent of the data ($\mathbf{d}$). Therefore, our proposed method can be implemented in a variety of modulation schemes, including the adaptive schemes presented in [31], [32].

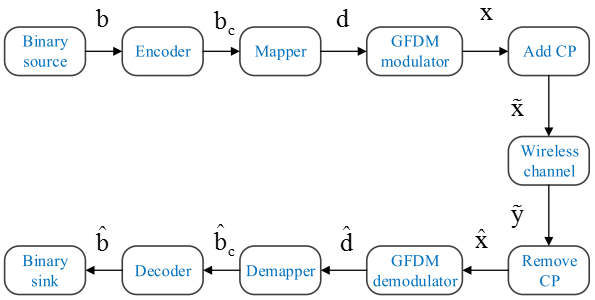

FIGURE 2. Block diagram of GFDM system.

III. SELF-INTERFERENCE IN GFDM

$\mathbf{d}$ is the QAM modulation data vector of order $N \times 1$ and can be expressed as follow:

$$\mathbf{d} = [d_{0,0}, \cdots, d_{K-1,0}, \ d_{0,1}, \cdots, d_{K-1,M-1}]^T. \tag{4}$$

At the receiver side, the received signal $\mathbf{y}$ is given by:

$$\mathbf{y} = \mathbf{H}\mathbf{x} + \mathbf{n}, \tag{5}$$

where $\mathbf{n}$ is additive white Gaussian noise (AWGN) with zero mean and variance σ_n^2. We show this as $\mathbf{n} \sim \mathcal{N}(0, \sigma_n^2)$. If we assume the communication channel is AWGN, then $\mathbf{H}$ becomes an identity matrix.[1] Applying MF to the receiver, the demodulation signal $\mathbf{z} = \hat{\mathbf{d}}$ can be expressed as follows:

$$\mathbf{z} = \mathbf{A}^H \mathbf{y} = \mathbf{A}^H \mathbf{A}\mathbf{d} + \mathbf{A}^H \mathbf{n} = \mathbf{B}\mathbf{d} + \mathbf{n}', \tag{6}$$

where $(.)^H$ denotes Hermitian conjugate, $\mathbf{A}^H$ shows MF in matrix form and $\mathbf{B} = \mathbf{A}^H \mathbf{A}$. To represent the self-interference in GFDM, we decompose matrix $\mathbf{B}$ as follows:

$$\begin{aligned} \mathbf{z} &= \mathbf{B}\mathbf{d} + \mathbf{n}' \\ &= (\mathbf{I}_N + \mathbf{B}_i).\mathbf{d} + \mathbf{n}' \\ &= \mathbf{d} + \underbrace{\mathbf{B}_i \mathbf{d}}_{\text{interference}} + \mathbf{n}' \\ &= \mathbf{d} + (\underbrace{\mathbf{B}_{In}}_{\substack{\text{Inband} \\ \text{interference}}} + \underbrace{\mathbf{B}_{Ad}}_{\substack{\text{Adjacent} \\ \text{interference}}})\mathbf{d} + \mathbf{n}', \end{aligned} \tag{7}$$

where $\mathbf{B}_i$ is off-diagonal part of $\mathbf{B}$ and represents interference from other symbols. $\mathbf{B}_{In}$ and $\mathbf{B}_{Ad}$ show inband interference and adjacent sub-carriers interference, respectively. $\mathbf{I}_N$ denotes identity matrix with order N.

[1] Our results can be extended to more complex wireless channel scenarios with slight modifications. The purpose of this article is to explain the main idea, provide the mathematical expressions and present the results in a most comprehensive way.

$$\mathbf{A} = \begin{bmatrix} g_{0,0}[0] & \cdots & g_{K-1,0}[0] & g_{0,1}[0] & \cdots & g_{K-1,M-1}[0] \\ g_{0,0}[1] & \cdots & g_{K-1,0}[1] & g_{0,1}[1] & \cdots & g_{K-1,M-1}[1] \\ \vdots & \cdots & \vdots & \vdots & \cdots & \vdots \\ g_{0,0}[N-1] & \cdots & g_{K-1,0}[N-1] & g_{0,1}[N-1] & \cdots & g_{K-1,M-1}[N-1] \end{bmatrix} \tag{3}$$

In GFDM, orthogonality between sub-carriers is lost due to the cyclic pulse shaping filters. To better understand the self-interference in GFDM, we rewrite (3) as equation (8), as shown at the bottom of the page. The signal can be recovered at the receiver using the MF. We have represented the received signal using (9), as shown at the bottom of the page. In this equation, $\{.\}^*$ denotes the complex conjugation. As shown in (9), there are two types of self-interference in GFDM:

1) **Inband interference:** interference between m and m' symbols in the same frequency due to the non-orthogonality shape of the shifted pulses ($g[n]$).
2) **Adjacent sub-carriers interference:** interference from adjacent sub-carriers $k'-1$ and $k'+1$ to k^{th} sub-carrier due to OOB caused by the proximity of these sub-carriers.

In this paper, we propose a general solution to reduce the impact of self-interference in GFDM systems. We use the SIC method in the symbol-frequency domain and eliminate the effects of these two types of self-interference independently. Based on these self-interferences, we present our proposed method with three modes. Mode-I is used when both inband and adjacent subcarrier interferences are present. We can use Mode- II and III when the system suffers only from adjacent subcarrier interference and inband interference, respectively. The different modes require different amounts of computational resources.

Now to describe (9) to show all types of interference in an (k, m) position, consider an example with $M = 5$, $K = 8$, and $\hat{d}_{3,2}$ as follows:

$$\hat{d}_{3,2} = d_{3,2} + \sum_{\substack{m=0 \\ m\neq m'}}^{5-1} \Bigg(\underbrace{g_{3,2}^{H}.g_{3,m}.d_{3,m}}_{\text{Inband Interference}} + \underbrace{g_{3,2}^{H}.g_{2,m}.d_{2,m} + g_{3,2}^{H}.g_{4,m}.d_{4,m}}_{\text{Adjacent Sub-carriers Interference}} \Bigg) + n', \tag{10}$$

where $d_{3,2}$ is desired input in the (3,2) position, $g_{3,2}^{H}.g_{3,m}.d_{3,m}$ denotes inband interference, $g_{3,2}^{H}.g_{2,m}.d_{2,m}$ and $g_{3,2}^{H}.g_{4,m}.d_{4,m}$ denotes adjacent sub-carriers interferences from sub-carriers 2 and 4.

To better clarify (10), we use Fig. 3 with $M = 5$ and $K = 8$. In Fig. 3. (a), the vertical and horizontal axes show the sub-carriers and the sub-symbols position, respectively. The location of the desired input $d_{3,2}$, the inband interference ($d_{3,0}, d_{3,1}, d_{3,3}, d_{3,4}$) and adjacent sub-carriers interferences from $k = 2$ and $k = 4$ are also depicted. Fig. 3. (b) shows the desired input and self-interferences values. To illustrate the interferences in more details, sub-symbols marked with red color represent the inband interference and the blue color represent the adjacent sub-carriers interferences.

IV. ANALYTICAL EXPRESSIONS

In this section, we derive analytical expressions to evaluate the BER of the system. Based on Eq. (9), since the self-interference factor is the linear composition of the random variables with i.i.d distributions, the self-interference factor can be modeled by Gaussian distribution as follows:

$$\hat{d}_{k',m'} = d_{k',m'} + I + n', \tag{11}$$

where I denotes the self-interference factor that can be decomposed as $I = I_r + jI_q$. I_r and I_q denote the real and imaginary parts of the self-interference factor, respectively. In Fig. 4, we have shown the distribution of the real and imaginary parts of the self interferences for $M = 5$, $K = 64$, and 64-QAM modulation. A raised cosine (RC) prototype filter with the roll-off factor $\alpha = 0.3$ is used. As shown in this figure the distributions are Gaussian and the analytical results match well with that of the simulations. Mathematically, the results are justified according to the central limit theorem [33]. The complex Gaussian approximation of the self-interference factor can be expressed

$$\mathbf{A} = [\underbrace{g_{0,0}[n]\cdots g_{K-1,0}[n]}_{\text{Sub-set of sub-symbol 0}} \mid \underbrace{g_{0,1}[n]\cdots g_{K-1,1}[n]}_{\text{Sub-set of sub-symbol 1}} \mid \underbrace{g_{0,M-1}[n]\cdots g_{K-1,M-1}[n]}_{\text{Sub-set of sub-symbol } M-1}]. \tag{8}$$

$$\begin{aligned}
\hat{d}_{k',m'} &= \sum_{n=-\infty}^{\infty} g_{k',m'}^{*}[n]\Bigg\{\sum_{m=0}^{M-1}\sum_{k=0}^{K-1} d_{k,m}g_{k,m}[n]\Bigg\} + n' \\
&= d_{k',m'}\Bigg\{\sum_{n=-\infty}^{\infty} g_{k',m'}^{*}[n]g_{k',m'}[n]\Bigg\} + \sum_{\substack{m=0 \\ (m,k)\neq(m',k')}}^{M-1}\sum_{k=0}^{K-1} d_{k,m}\Bigg\{\sum_{n=-\infty}^{\infty} g_{k',m'}^{*}[n]g_{k,m}[n]\Bigg\} + n' \\
&= d_{k',m'}.\underbrace{g_{k',m'}^{H}.g_{k',m'}}_{1} + \sum_{\substack{m=0 \\ (m,k)\neq(m',k')}}^{M-1}\sum_{k=0}^{K-1} g_{k',m'}^{H}.g_{k,m}.d_{k,m} + n' \\
&= d_{k',m'} + \sum_{\substack{m=0 \\ m\neq m'}}^{M-1} \Bigg(\underbrace{g_{k',m'}^{H}.g_{k',m}.d_{k',m}}_{\text{Inband Interference}} + \underbrace{g_{k',m'}^{H}.g_{k'-1,m}.d_{k'-1,m} + g_{k',m'}^{H}.g_{k'+1,m}.d_{k'+1,m}}_{\text{Adjacent Sub-carriers Interference}} \Bigg) + n'.
\end{aligned} \tag{9}$$

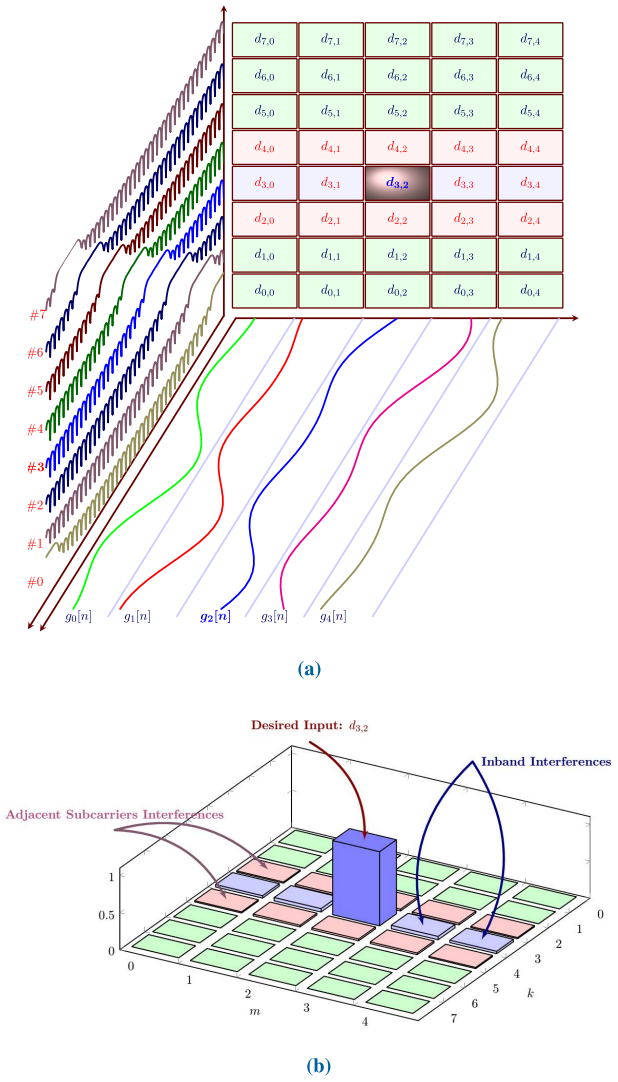

FIGURE 3. Self-interference in GFDM systems ($M = 5$, $K = 8$). (a) desired input and self-interferences location; (b) desired input and self-interferences values.

as follows:

$$I_r \sim \mathcal{N}(0, \frac{N_I}{2}),\ I_q \sim \mathcal{N}(0, \frac{N_I}{2})$$
$$\Rightarrow f_I(i) = \frac{1}{\pi N_I} e^{-|i|^2/N_I}, \tag{12}$$

where N_I denotes the variance of self-interference factor. In this work, we assume that the mean of the data is zero. Consequently, the mean of the self-interference factor will be zero and N_I can be calculated based on (9) as follows:

$$N_I = E_s \sum_{\substack{m=0 \\ m\neq m'}}^{M-1} \Big(|g^H_{k',m'} \cdot g_{k',m}|^2 + |g^H_{k',m'} \cdot g_{k'-1,m}|^2 + |g^H_{k',m'} \cdot g_{k'+1,m}|^2 \Big), \tag{13}$$

where E_s denotes the variance of data.

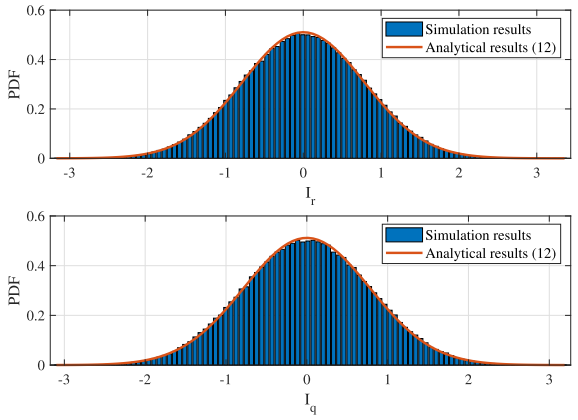

FIGURE 4. Real and imaginary distributions of self-Interference for $M = 5$, $K = 64$ and 64-QAM modulation.

In this work, q-ary QAM (q-QAM) with $q = 2^{2k}$ is considered, hence, the probability of error can be expressed as follows [34]:

$$P_e = 4(1 - \frac{1}{\sqrt{M}})Q(\sqrt{\frac{3\log_2 M \times E_b}{(M-1)(N_I + N_0)}} \times \big(1 - (1 - \frac{1}{\sqrt{M}})\big)Q(\sqrt{\frac{3\log_2 M \times E_b}{(M-1)(N_I + N_0)}}, \tag{14}$$

where N_0 denotes the variance of the noise and $E_b = \frac{E_s}{\log_2 M}$.

V. SELF-INTERFERENCE CANCELLATION METHOD

As mentioned in Section II, the MF receiver is unable to remove the intrinsic self-interference [26]. In this research, we use an SIC-based technique to remove the interferences from the received signal. In our SIC technique, there are two phases: first, the interference factor ($\mathbf{B}_i = \mathbf{B} - \mathbf{I}_N$) is calculated, and in the second phase, the interference is removed from the received signal. We describe the process in Algorithm 1. In the following, we will explain our proposed method in more detail.

Our proposed SIC technique can operate in three modes according to the self-interferences types described in Section III. If SIC operates in Mode-I, it will remove both inband and adjacent sub-carrier interferences. If it operates in Mode-II, the SIC only removes the corresponding inband self-interference and in Mode-III, it removes the subcarrier interferences. Mode-II and III are provided to reduce the system complexity. Considering these modes, the GFDM system can be implemented using one of the following structures:

1) Conventional GFDM system: in this case, GFDM uses a regular prototype filter so that both inband and adjacent sub-carrier interferences are present. In this case, all or part of the interferences can be removed to achieve an acceptable performance limit. Depending on the performance limit and requirement, the system can be operated in Mode I, II, or III.

2) A GFDM system with a high-performance prototype filter: in this case, the system suffers mainly from one of the interferences, inband or adjacent sub-carrier. However, these interferences can be removed with Mode-II or III with less computational complexity compared to Mode-I.

Algorithm 1 Proposed SIC Algorithm

iteration j=1, 2, ..., J

Phase 1:
- 1) Using the maximum likelihood (ML) method: $\mathbf{z}_j \rightarrow \hat{\mathbf{s}}$
- 2) Using demodulation: $\hat{\mathbf{s}} \rightarrow \hat{\mathbf{d}}$
- 3)
  - Mode I : $\mathbf{B}_i = \mathbf{B}_{In} + \mathbf{B}_{Ad}$
  - Mode II : $\mathbf{B}_i = \mathbf{B}_{Ad}$
  - Mode III : $\mathbf{B}_i = \mathbf{B}_{In}$
- 4) Interference calculation: $\mathbf{F}_i = \mathbf{B}_i\hat{\mathbf{d}}$

Phase 2:
- 4) $\mathbf{z}_{j+1} = \mathbf{z}_j - \mathbf{F}_i$
- 5) Repeat step 1 to 4

In Algorithm 1, first we use maximum likelihood (ML) method to estimate $\hat{\mathbf{s}}$ from $\mathbf{z}_j$, where $\mathbf{z}_j$ denotes MF output in iteration j. We estimate $\hat{\mathbf{d}}$ values from $\hat{\mathbf{s}}$ and then calculate the interference $\mathbf{F}_i$. Following that we subtract the interference from $\mathbf{z}_j$ to eliminate the interference.

In the proposed method, the complexity of the GFDM when operates in Mode II or III is substantially less than cases when the system operates in Mode I. By using orthogonal pulse shapes (g[n]) such as Discrete Prolate Spheroidal Sequences (DPSS) [35], inband interference is inherently removed and, hence, Mode-II can be used to cancel the remaining interferences. If the GFDM system uses a dual-filter method at the receiver [26], the self-interference of the adjacent sub-carriers will be considerably low. Therefore, the system can operate based on Mode-III.

TABLE 1. Different mode types.

Mode	Interference Type	Conditions
Mode-I	Inband and djacent sub-carriers	Conventional GFDM
Mode-II	Adjacent sub-carriers	Orthogonal pulse shapes or DPSS [35]
Mode-III	Inband	Dual filter [26]

To better illustrate the proposed idea of the operation modes in GFDM, we use Fig. 5 with $M = 5$ and $K = 8$. In Fig. 5. (a) we show Mode-I and its interferences. In Fig. 5. (b) and (c), Mode- II and Mode- III are shown with their corresponding interferences. To illustrate the interferences, the sub-symbols marked with red color represent the inband interferences and the blue color represents the interferences of the adjacent sub-carriers.

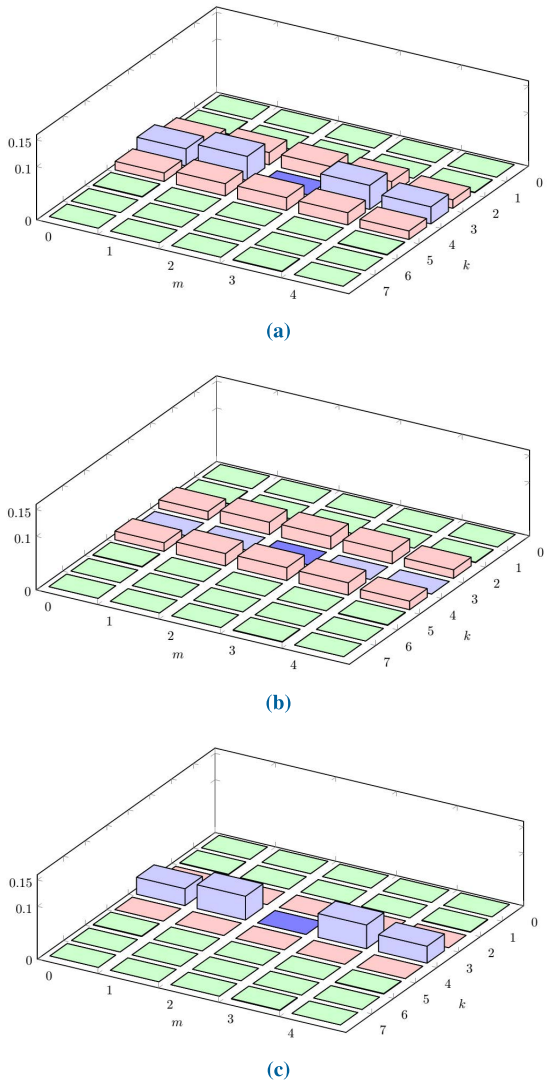

FIGURE 5. The proposed modes ($M = 5$, $K = 8$). (a) Mode-I; (b) Mode-II; (c) Mode-III.

VI. NUMERICAL RESULTS

In this section, we evaluate the BER performance of ZF and MF with the proposed SIC-based receivers in mode I for conventional GFDM using analytical results and numerical simulations. The simulation parameters are shown in Table 1 based on [27], [28].

In Fig. 6, we compare the BER performance of the GFDM system with different receiver implementations for the different number of iterations ($J = 1, 2, 3$) for each SIC receiver. As a benchmark, our results also compare the system performance with the ZF technique. In these simulations, $K = 32$ sub-carriers and $M = 5$ sub-symbols are considered. An RC prototype filter with the roll-off factor $\alpha = 0.3$ is used. As shown in this figure, our proposed SIC technique outperforms the SIC technique in [28]. Our SIC-based receiver also outperforms the ZF receiver after only 3 iterations.

We also validate our analytical findings using computer simulations in Fig. 7. In these simulations, $K = 64$ sub-carriers and $M = 5$ sub-symbols. An RC prototype filter

TABLE 2. GFDM simulation parameters.

Parameters	Value
Modulation scheme	64, 256-QAM
Sub-symbols (M)	5, 7
Sub-carriers (K)	32, 64
Null sub-carriers (K_n)	2, 15
Roll-off factor (α)	0.3
Channel	AWGN

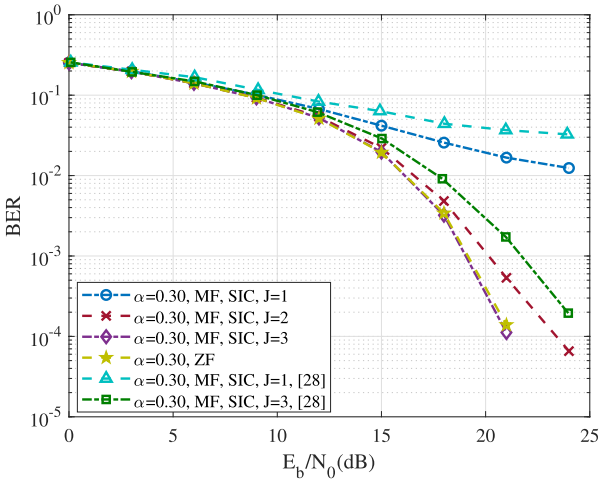

FIGURE 6. BER performance for $M = 5$, $K = 32$, 64-QAM modulation, and RC prototype filter.

with the roll-off factor $\alpha = 0.3$ is utilized. As shown in this figure, the results from our analytical derivations are in good agreement with that of the simulation results.

Fig. 8 shows the performance of the GFDM-MF receiver in different iterations. In this simulation, $K = 32$ sub-carriers and $M = 7$ sub-symbols. As shown in this figure, our proposed SIC receiver with 5 iterations archives the same performance as the GFDM-ZF receiver. The proposed method outperforms GFDM-ZF at iteration 6.

To verify the performances of the GFDM system with the proposed SIC technique, we analyze the signal to interference ratio (SIR) parameter. For this simulation, we use an RC prototype filter with the roll-off factor 0.3, $K = 64$ sub-carriers and $M = 7$ sub-symbols. The SIR simulation results are shown in Fig. 9. Observe that after 1 iteration at SNR= 15 dB, the SIR value improves significantly and after 4 iterations it reaches 40.43 dB. In SNR= 20 dB, after 2 iterations, the interference ratio reaches zero and the SIR value approaches infinity.

As shown in Fig. 9, the performance of the system increases from 15 dB to 30 dB after one iteration. In our algorithm, we utilize the modulation matrix $\mathbf{A}$ which is assumed to be known at the receiver. Therefore, in the first iteration, we have been able to remove most of the self-interference in

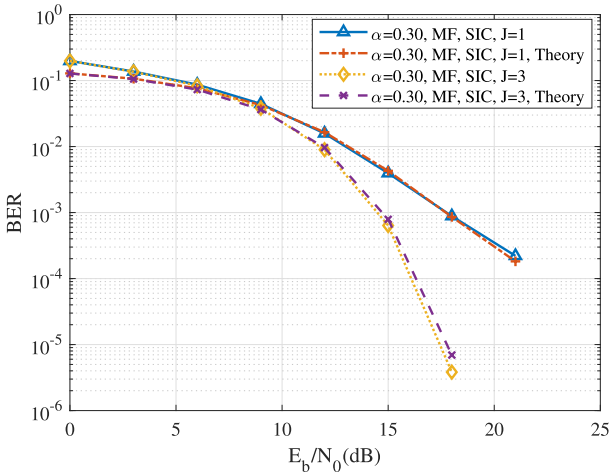

FIGURE 7. Comparison of analytical and simulation results.

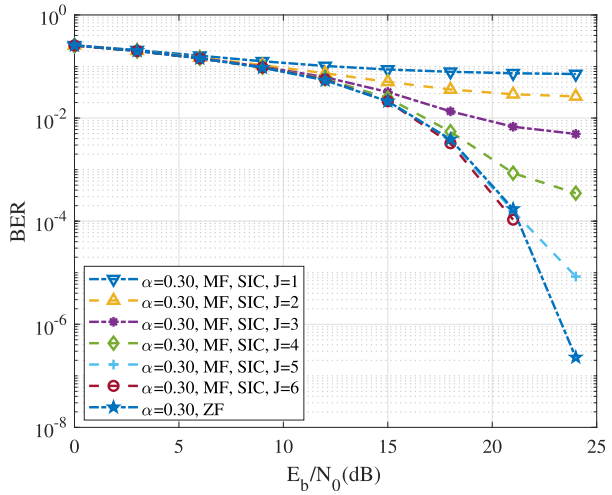

FIGURE 8. BER performance for $M = 7$, $K = 32$, 256-QAM modulation, and RC prototype filter.

the first iteration and gradually reach a steady state. However, in low SNR scenarios, due to high noise volume, perfect elimination of self-interferences will be challenging if not impossible.

A. SNIR ANALYSIS

Now, we analyze the SNIR by considering inband and adjacent sub-carriers self-interferences. The SNIR is given by:

$$SINR(j) = \frac{P_s}{N_I(j) + N_0}, \tag{15}$$

where P_s is the average energy per data, j is the number of iteration. The variance of the self-interference factor is calculated based on (13), and the variance of the noise is $N_0 = \sigma_n^2$. According to (15), when $N_I \to 0$, SINR $\to$ SNR which leads to convergence.

To evaluate (15), we illustrate the SNIR performance of conventional GFDM in Mode-I in Fig. 10. According to (15) and Fig. 10, increasing the number of iterations decreases the

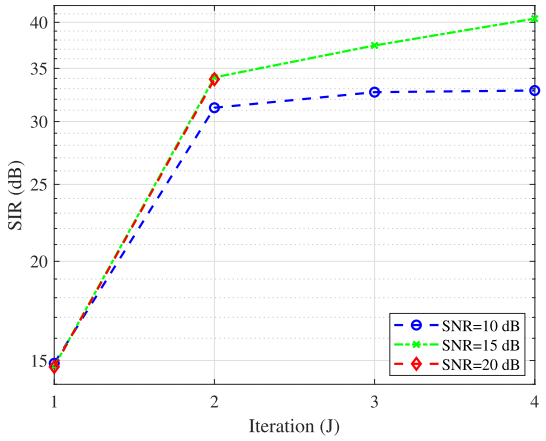

FIGURE 9. The SIR of the proposed method in different iterations for $M = 7$, $K = 64$, 256-QAM modulation, and RC prototype filter.

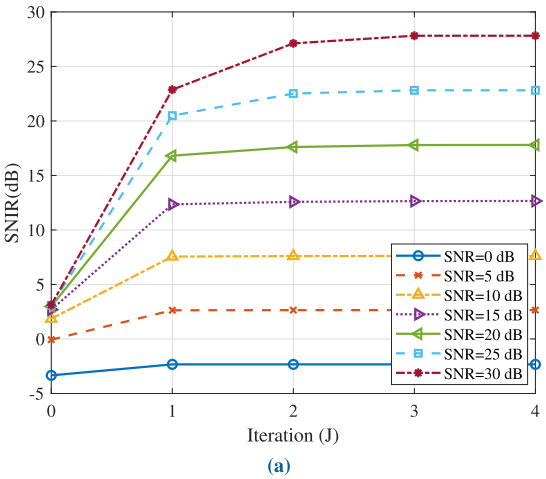

(a)

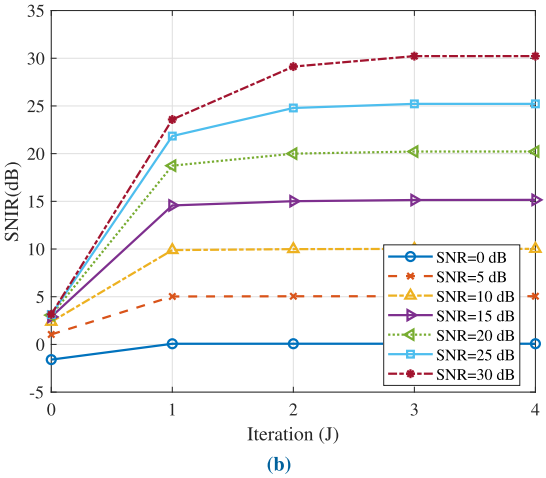

(b)

FIGURE 10. The SNIR of the proposed method in different iterations for $M = 7$, $K = 64$, 256-QAM modulation, and RC prototype filter with $\alpha = 0.3$; a) $K_n = 2$ b) $K_n = 15$.

self-interference factor, leading to an increase in SNIR and convergence to SNR. The reason for the lack of convergence to the SNR value is the error-induced self-interference. This error-induced self-interference cannot be completely reduced to zero unless we control it with parameters such as the modulation type and the number of null sub-carriers to bring the SNIR closer to the SNR value as shown in Fig. 10. b.

TABLE 3. The complexity of different GFDM techniques.

Techniques	Number of multiplications
GFDM-OQAM [25]	$4N^2$
GFDM-DF [26]	$2N^2$
SIC in [27], [28]	$MN(\log_2 MN + \log_2 M + 1)$ $+J(2MN \log_2 M + MN)$
Iterative in [29]	$JN[(8N^2 - 4NK - 8N + 2K$ $+2)(\frac{q}{2})^{N-1} + 2N^2 - 8N + 6]$
Proposed SIC	Mode I $\Rightarrow JN(3M-1)$ Mode II $\Rightarrow JN(2M)$ Mode III $\Rightarrow JN(M-1)$

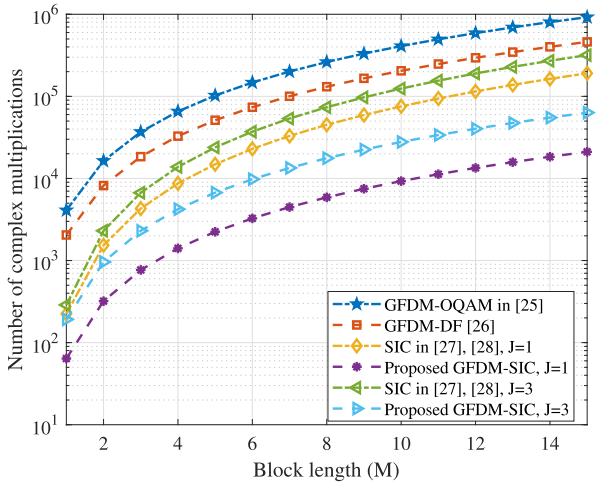

FIGURE 11. Computational complexity of different techniques for $K = 32$.

B. COMPLEXITY ANALYSIS

We summarize the computational complexity analysis results of GFDM receivers in terms of the number of complex multiplications in Table 3. GFDM with DF receiver has two parts, the matrix dimension of each part is $N \times \frac{N}{2}$. Therefore, the GFDM-DF complexity is similar to the conventional GFDM system. The GFDM-OQAM separately transmits the real and imaginary parts of the data symbol, therefore, its computational complexity is twice that of the MF receiver. Considering that the proposed algorithm in [29] performs message computations iteratively, its computational complexity is $\mathcal{O}(c^N)$. In contrast, in our proposed method, computational complexity has a linear relation with N (see Table 3).

The complexity of GFDM systems with the proposed SIC scheme and other receivers is compared in Fig. 11. In this analysis, $K = 32$ sub-carriers and $J = 1, 3$ iteration are considered. The complexity of GFDM-OQAM and GFDM-DF is too high compared to the proposed GFDM-SIC scheme.

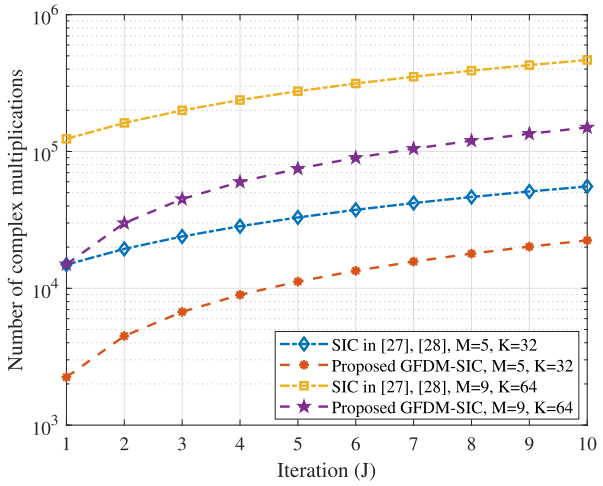

FIGURE 12. Computational complexity comparison for different iterations.

Compared to GFDM-SIC [27], [28], the proposed GFDM-SIC has lower computational complexity. Moreover, our proposed technique has the best performance among all other GFDM techniques. The complexity of different GFDM-SIC techniques for different iterations is shown in Fig. 12. The proposed GFDM-SIC has low computational complexity compared to the SIC receiver in [27], [28]. Therefore, the proposed GFDM based on the proposed SIC scheme is a better choice, especially for the case where there are larger block lengths in a GFDM system.

VII. CONCLUSION

GFDM is one of the candidate waveforms for 5G wireless cellular networks. In this paper, we studied GFDM systems and proposed a new system model along with an SIC technique to eliminate self-interference with low complexity. For the first time, in this paper, we introduce a GFDM system model that defines two types of independent self-interferences namely, inband and adjacent sub-carriers interferences. Building on this idea, we came up with an SIC and signal estimation technique that outperforms the GFDM-SIC counterparts. We analytically verified the performance of the proposed technique by approximating the system self-interference using Gaussian distribution and obtained the probability of error in presence of noise. We presented numerical results that justify the use of Gaussian distribution to approximate self-interference in our model. We have shown that the results from our analytical derivations match well with that of the computer simulations. As shown in our results, not only our method is able to reduce the system complexity but also it exhibits a better performance in terms of BER and SIR compared to its existing counterparts.

REFERENCES

[1] V. Kumar and N. B. Mehta, "Exploiting correlation with wideband CQI and making differential feedback overhead flexible in 4G/5G OFDM systems," *IEEE Trans. Wireless Commun.*, vol. 20, no. 4, pp. 2579–2591, Apr. 2021.

[2] J. A. C. Bingham, "Multicarrier modulation for data transmission: An idea whose time has come," *IEEE Commun. Mag.*, vol. 28, no. 5, pp. 5–14, May 1990.

[3] S. Chen and J. Zhao, "The requirements, challenges, and technologies for 5G of terrestrial mobile telecommunication," *IEEE Commun. Mag.*, vol. 52, no. 5, pp. 36–43, May 2014.

[4] R. A. Kumar and K. S. Prasad, "Performance analysis of GFDM modulation in heterogeneous network for 5G NR," *Wireless Pers. Commun.*, vol. 116, no. 3, pp. 2299–2319, Feb. 2021.

[5] M. R. Ghavidel Aghdam, J. Deiri, B. Mozaffari Tazehkand, and R. Abdolee, "A low complex peak-to-average power ratio reduction in orthogonal frequency division multiplexing systems using a two-dimensional interleaving strategy," *Int. J. Commun. Syst.*, vol. 33, Sep. 2020, Art. no. e4622.

[6] P. Banelli, S. Buzzi, and G. Colavolpe, "Modulation formats and waveforms for 5G networks: Who will be the heir of OFDM?: An overview of alternative modulation schemes for improved spectral efficiency," *IEEE Signal Process. Mag.*, vol. 31, no. 6, pp. 80–93, Oct. 2014.

[7] G. Wunder, P. Jung, M. Kasparick, T. Wild, F. Schaich, Y. Chen, S. T. Brink, I. Gaspar, N. Michailow, A. Festag, and L. Mendes, "5G NOW: Non-orthogonal, asynchronous waveforms for future mobile applications," *IEEE Commun. Mag.*, vol. 52, no. 2, pp. 97–105, Feb. 2014.

[8] M. Matthe, N. Michailow, I. Gaspar, and G. Fettweis, "Influence of pulse shaping on bit error rate performance and out of band radiation of generalized frequency division multiplexing," in *Proc. IEEE Int. Conf. Commun. Workshops (ICC)*, Jun. 2014, pp. 43–48.

[9] H. Lin and P. Siohan, "An advanced multi-carrier modulation for future radio systems," in *Proc. IEEE Int. Conf. Acoust., Speech Signal Process. (ICASSP)*, May 2014, pp. 8097–8101.

[10] Y. Ma, N. Wu, J. A. Zhang, B. Li, and L. Hanzo, "Generalized approximate message passing equalization for multi-carrier faster-than-Nyquist signaling," *IEEE Trans. Veh. Technol.*, vol. 71, no. 3, pp. 3309–3314, Mar. 2022.

[11] Y. Ma, N. Wu, J. A. Zhang, B. Li, and L. Hanzo, "Parametric bilinear iterative generalized approximate message passing reception of FTN multi-carrier signaling," *IEEE Trans. Commun.*, vol. 69, no. 12, pp. 8443–8458, Dec. 2021.

[12] H.-F. Wang, F.-B. Ueng, Y.-S. Shen, and K.-X. Lin, "Low-complexity receivers for massive MIMO-GFDM communications," *Trans. Emerg. Telecommun. Technol.*, vol. 32, no. 4, 2021, Art. no. e4219.

[13] G. Fettweis, M. Krondorf, and S. Bittner, "GFDM–Generalized frequency division multiplexing," in *Proc. VTC Spring IEEE 69th Veh. Technol. Conf.*, Apr. 2009, pp. 1–4.

[14] V. Vakilian, T. Wild, F. Schaich, S. ten Brink, and J.-F. Frigon, "Universal-filtered multi-carrier technique for wireless systems beyond LTE," in *Proc. IEEE Globecom Workshops (GC Wkshps)*, Dec. 2013, pp. 223–228.

[15] N. Michailow and G. Fettweis, "Low peak-to-average power ratio for next generation cellular systems with generalized frequency division multiplexing," in *Proc. Int. Symp. Intell. Signal Process. Commun. Syst.*, Nov. 2013, pp. 651–655.

[16] S. M. J. A. Tabatabaee, M. Rajabzadeh, and M. Towliat, "A novel low-complexity GFDM relay communication system: Relay selection and filter-and-forward," *IEEE Trans. Signal Process.*, vol. 69, pp. 5147–5158, 2021.

[17] E. Catak, A. Moldsvor, and M. Derawi, "Transceiver design for GFDM with hexagonal time–frequency allocation using the polyphase decomposition," *Electronics*, vol. 9, no. 11, p. 1862, Nov. 2020.

[18] M. Q. Khan and M. D. Nisar, "Spatial transmit diversity for GFDM via low complexity transceiver design," in *Proc. IEEE 93rd Veh. Technol. Conf. (VTC-Spring)*, Apr. 2021, pp. 1–5.

[19] S. F. Caglayan, M. Isbit, S. Ilgun, and E. Erdogan, "Design and comparison of GFDM receivers for 5G communication systems," in *Proc. 28th Signal Process. Commun. Appl. Conf. (SIU)*, Oct. 2020, pp. 1–4.

[20] S. M. J. A. Tabatabaee, M. Towliat, and M. Rajabzadeh, "Novel transceiver beamforming schemes for a MIMO-GFDM system," *Phys. Commun.*, vol. 47, Aug. 2021, Art. no. 101376.

[21] W. D. Dias, L. L. Mendes, and J. J. P. C. Rodrigues, "Low complexity GFDM receiver for frequency-selective channels," *IEEE Commun. Lett.*, vol. 23, no. 7, pp. 1166–1169, Jul. 2019.

[22] F. T. Miandoab and B. M. Tazehkand, "NOMA performance enhancement-based imperfect SIC minimization using a novel user pairing scenario involving three users in each pair," *Wireless Netw.*, vol. 26, no. 5, pp. 3735–3748, Jul. 2020.

[23] X. Zhang, Z. Wang, X. Ning, and H. Xie, "On the performance of GFDM assisted NOMA schemes," *IEEE Access*, vol. 8, pp. 88961–88968, 2020.

[24] Y. Lin, Z. Yang, and H. Guo, "Energy-efficient resource allocation in downlink GFDM-NOMA networks," in *Proc. 11th Int. Conf. Wireless Commun. Signal Process. (WCSP)*, Oct. 2019, pp. 1–7.
[25] I. Gaspar, M. Matthe, N. Michailow, L. L. Mendes, D. Zhang, and G. Fettweis, "Frequency-shift offset-QAM for GFDM," *IEEE Commun. Lett.*, vol. 19, no. 8, pp. 1454–1457, Aug. 2015.
[26] F. Li, K. Zheng, L. Zhao, H. Zhao, and Y. Li, "Design and performance of a novel interference-free GFDM transceiver with dual filter," *IEEE Trans. Veh. Technol.*, vol. 68, no. 5, pp. 4695–4706, May 2019.
[27] I. Gaspar, N. Michailow, A. Navarro, E. Ohlmer, S. Krone, and G. Fettweis, "Low complexity GFDM receiver based on sparse frequency domain processing," in *Proc. IEEE 77th Veh. Technol. Conf. (VTC Spring)*, Jun. 2013, pp. 1–6.
[28] A. Rezazadehreyhani, A. Farhang, and B. Farhang-Boroujeny, "Circularly pulse-shaped waveforms for 5G: Options and comparisons," in *Proc. IEEE Global Commun. Conf. (GLOBECOM)*, Dec. 2014, pp. 1–7.
[29] I. B. F. de Almeida, G. P. Aquino, and L. L. Mendes, "Iterative receiver for non-orthogonal waveforms based on the sum-product algorithm," in *Proc. 16th Int. Symp. Wireless Commun. Syst. (ISWCS)*, Aug. 2019, pp. 38–42.
[30] N. Michailow, M. Matthe, I. S. Gaspar, A. N. Caldevilla, L. L. Mendes, A. Festag, and G. Fettweis, "Generalized frequency division multiplexing for 5th generation cellular networks," *IEEE Trans. Commun.*, vol. 62, no. 9, pp. 3045–3061, Sep. 2014.
[31] T. A. Almohamad, M. F. M. Salleh, M. N. Mahmud, I. R. Karas, N. S. M. Shah, and S. A. Al-Gailani, "Dual-determination of modulation types and signal-to-noise ratios using 2D-ASIQH features for next generation of wireless communication systems," *IEEE Access*, vol. 9, pp. 25843–25857, 2021.
[32] T. A. Almohamad, M. Salleh, M. N. Mahmud, A. H. Y. Saaed, and S. A. Al-Gailani, "Automatic modulation recognition in wireless communication systems using feature-based approach," in *Proc. 10th Int. Conf. Robot., Vis., Signal Process. Power Appl.*, 2019, pp. 403–409.
[33] B. Avanzi, G. B. Beaulieu, P. L. de Micheaux, F. Ouimet, and B. Wong, "A counterexample to the existence of a general central limit theorem for pairwise independent identically distributed random variables," *J. Math. Anal. Appl.*, vol. 499, no. 1, Jul. 2021, Art. no. 124982.
[34] J. G. Proakis and M. Salehi, *Digital Communications*. New York, NY, USA: McGraw-Hill, 2008.
[35] S. K. Bandari, V. V. Mani, and A. Drosopoulos, "Multi-taper implementation of GFDM," in *Proc. IEEE Wireless Commun. Netw. Conf.*, Apr. 2016, pp. 1–5.

BEHZAD MOZAFFARI TAZEHKAND was born in Iran, in 1968. He received the B.S. degree from the University of Tabriz, Tabriz, Iran, in 1993, the M.S. degree from the K. N. Toosi University of Technology, in 1996, and the Ph.D. degree from the University of Tabriz, in 2006. He is currently a Professor with the Faculty of Electrical and Computer Engineering, University of Tabriz. He has authored or coauthored more than 93 research papers, including journal articles, book chapters, conference proceedings, and workshops. His research interest includes wireless communication. He is currently working on multi-carrier modulations for 5G networks and future mobile communication systems.

MOHAMMAD REZA GHAVIDEL AGHDAM received the B.S. degree in electrical engineering from Urmia University, in 2014, and the M.S. degree in communication engineering and the Ph.D. degree in telecommunication engineering from the University of Tabriz, Tabriz, Iran, in 2016 and 2020, respectively. He is currently working as a Researcher pursuing both academic and research work with the Wireless Communication Laboratory, University of Tabriz. His research interests include signal processing, massive-MIMO, millimeter wave, NOMA, OFDM and GFDM systems, and machine learning.

VIDA VAKILIAN received the Ph.D. degree in electrical engineering from the Ecole Polytechnique de Montreal, QC, Canada, in 2014. She is currently an Assistant Professor with California State University Channel Islands (CSUCI), CA, USA. From 2013 to 2014, she was a Co-Op Engineer at Inter Digital Communications Inc., where she worked on the design and development of advanced signal-processing algorithms for the 3rd Generation Partnership Project standards-based cellular systems. In 2012, she was a Research Intern with Bell Labs, Alcatel-Lucent, Germany. During this period, she contributed to the 5GNOW project, aiming to develop new robust PHY layer concepts, suited for future wireless systems. Her research interests include communication theory, statistical signal processing, and hardware design and integration.

REZA ABDOLEE received the Ph.D. degree in electrical and computer engineering from McGill University, Montreal, Canada, in 2014. After completing his Ph.D. degree, he worked as a Senior Wireless System Engineer at Qualcomm Inc. where he involved in the design and modeling of digital subsystems of modem chips used in smartphones and wireless devices. He is currently an Assistant Professor with the Department of Computer Science, California State University Channel Islands (CSUCI) and an Adjunct Professor with the University of California Santa Barbra (UCSB). His research interests include cybersecurity, wireless communication and signal processing with applications to Internet of Things (IoT), and industrial control systems (ICS).